Synthesization of Edge Noises for Touch Probe and Laser Sensor Measurement

Jie Shen

University of Michigan-Dearborn, shen@mich.edu

ABSTRACT

In this paper we investigate the spatial distribution of measurement noise at sharp edges. A local cylindrical coordinate system is used to decompose the measurement noise at sharp edges into to two components, magnitude and angle. The spatial distributions of these two components are analyzed at sharp edges for both touch probe and laser sensor. A new concept, statistical binary tree, is proposed for representing the spatial noise distribution on a sharp edge, and a synthesis simulator is proposed for accurate reproduction of measurement noise at sharp edges.

Keywords: Metrology, Quality Control, Laser Sensor, Touch Probe, Noise, Reverse Engineering.

1. INTRODUCTION

Measurement noise is an intrinsic problem with various existing touch probes and laser sensors. In particular, more severe measurement errors of various sensors are frequently observed near sharp edges of the objects that are being measured, as illustrated in Figure 1 in which σ refers to the standard deviation of measurement errors. In the past, different surface smoothing algorithms for sharp edges have been proposed [1-15], and the algorithms were compared on noisy surfaces generated by a very simple synthetic noise model controlled by a random number generator [15]. However, real measurement noise does not exactly follow the pattern prescribed by the random number generator. The question is whether or not we can design a more realistic measurement noise synthesizer as a standard reference to test different existing or new denoising algorithms.

There are many factors, including operator, material property, surface roughness, surface geometric properties, environment noise and sensor noise, which can contribute to the measurement noise of touch probes and laser sensors. In this paper, our focus is on the behavior of measurement noise as a whole in a laboratory environment without any extraordinary external influence and without abnormal operator mistakes. Although there were some studies on the simulation models of laser scanning probes [16-18], very little systematic studies have been conducted for revealing the behavior of measurement noises at sharp edges.

The objective of this paper is to explore the spatial distribution of measurement noise at sharp edges, and design a synthetic simulator for accurate description of measurement noise. The unique contributions of this paper include: 1) a local cylindrical coordinate decomposition of measurement noise at sharp edges; 2) a statistical binary tree for the representation of spatial distribution of noise magnitude at sharp edges; and 3) a synthetic noise simulator for the sharp edges.

The remaining of this paper is organized as follows. In Section 2, the exploration of spatial distribution of measurement noise at sharp edges is introduced. Then, the statistical behavior of such spatial distribution is reported and discussed in Section 3. Next in Section 4, the concepts of measurement noise templates and statistical binary trees are introduced. Finally, a synthetic noise simulator is developed for sharp edges in Section 5 and some concluding remarks are given in Section 6.

2. SPATIAL DISTRIBUTION OF MEASUREMENT NOISE AT SHARP EDGES

In this study we use standard metrology gage blocks with sharp edges as test specimens on which touch probes or laser scanners are applied. The surface roughness of these specimens is considered negligible (less than 0.6 micrometer), compared to the range of measurement noises of laser sensors (about 50 micrometers -- personal communication with Burt Mason, ROMER CimCore, Hexagon Metrology). Therefore, we assume that the sharp edges of these specimens are perfect without need for considering the surface roughness in the neighborhood of these edges.

The laser sensor used in this study is a Surveyor Laser Probe (SLP) made by Laser Design Inc. The data acquisition rate is 144,000 points per second, and the sample density ranges from 69 to 550 micrometers, which is

dense enough for the study of spatial distribution. After a point cloud is obtained by laser scanning, a sample density of 0.25 mm through 0.5 mm is used to extract information from the point cloud for the study of spatial distribution. The exact value of this second sample density is dependent upon the overall measurement size. The bigger the overall measurement size is, the sparser the second sample density should be. With a Renishaw touch probe, we tried to sample as fewer data points as possible, because its operation was manual at a very low data acquisition rate.

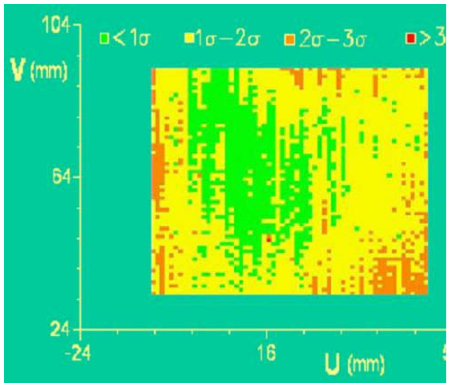

Fig. 1: A color image of measurement error distribution of a Hymarc 45C laser probe on a rectangular face of a calibration target without the inclusion of CMM volumetric error (Courtesy of Allan Spence, McMaster University).

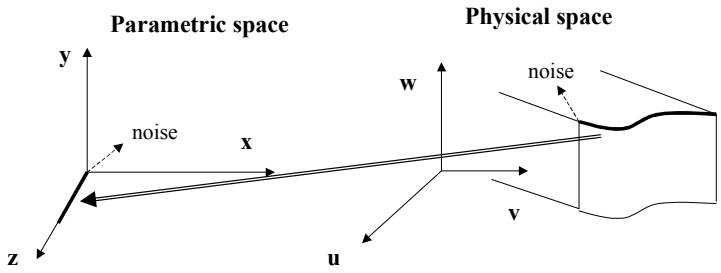

Fig. 2: Representation of measurement noise in a parametric space (transformation from a 3D sharp edge to a line segment).

The measurement noise on a 3D object generally occurs in three dimensions, and could be very difficult to determine in a general format. In this study, we focus on measurement noise at a given sharp edge in the plane that is perpendicular to the edge. To handle measurement noise at a sharp edge, the edge is converted to a line segment in *z* direction of a parametric space, in which the measurement noise at the edge can be represented by *x* and *y* axes in the parametric space, as shown in Figure 2. A sharp corner can be easily transformed to the origin in the parametric space with respect to measurement noise at the sharp corner. The noise at the origin takes a form of an arbitrary 3D vector in this parametric space.

We define the line segment in the parametric space together with the transformed noise as a *noise template*. This noise template, once created, can be applied onto arbitrary sharp edges by a process similar to texture mapping in computer graphics. We call this process a *noise template mapping*, which is then used as an effective tool to generate synthetic noise over synthetic object surfaces and edges. The size of the noise template depends upon the size of the original sample edge in the initial physical space.

Figure 3(a) shows a two-inch gage block with its top surface marked by grids. The maximum roughness, $R_{\max}$, of its surfaces is less than 0.18 micrometers. Therefore, the neighborhood around sharp edges can be approximately considered as a region without surface roughness. Each grid rectangle was used for one sampling measurement of a touch probe mounted on a CMM. A typical measurement noise of the touch probe on its top surface is illustrated in Figure 3(b), in which blue color is used for measurement noise and gray color is for regular grids on the top surface. The measurement on the edges were conducted on edge line segments of each grid rectangle adjacent to an edge, and the measurement at sharp corners were performed at the corner vertex of each grid rectangle adjacent to the corner, as illustrated in Figure 3(c). Since the dimensions of the block are much greater than the magnitude of measurement noises, micrometer scale is used for measurement noises and millimeter scale is for the grids in Figures 3(b).

The measurement noise of a laser probe is shown in Figure 3(d), in which pink color is used for edge noise and blue color for interior noise. The average magnitude of edge noise is one time greater than that of interior noise, and the average magnitude of corner noise is even higher than that at edges. This indicates the importance of an accurate denoising algorithm for sharp edges and corners with laser sensors.

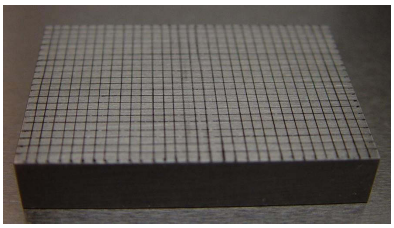

(a) a two-inch gage block

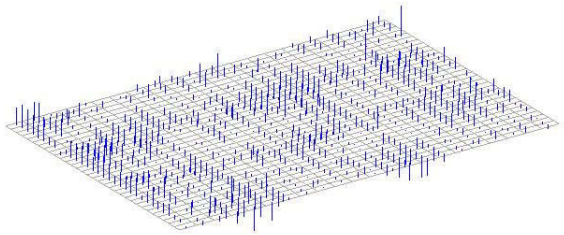

(b) scaled measurement noise of a touch probe

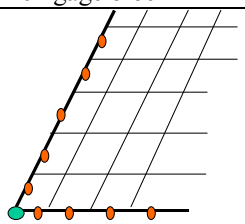

(c) sampling locations at sharp edges and corners with a touch probe (orange color – edge sample; green color – corner sample)

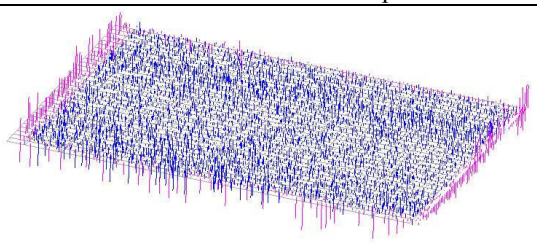

(d) scaled measurement noise of a laser probe (10 times enlargement in vertical direction; pink color – edge noise, magnitude = 81.9 micrometers; blue color – interior noise, magnitude = 39.5 micrometers; magnitude of corner noise = 91.4 micrometers)

Fig. 3: A gage block and the measured noises of a touch probe and a laser probe.

3. STATISTICAL BEHAVIOR OF SPATIAL DISTRIBUTION OF MEASUREMENT NOISE AT SHARP EDGES

From the viewpoint of statistics, we consider the following two aspects in modeling the measurement noise:

(a) The noise at each edge or corner point is considered as an independent random variable. This can be represented by the following equation:

$$(g_x, g_y, g_z) = (x, y, z) + (e_x, e_y, e_z)\,, \tag{1}$$

where (x, y, z) refers to the vector of a true surface point in a physical space, and (e_x, e_y, e_z) is a random perturbation vector at that point. (g_x, g_y, g_z) represents a perturbed position vector at the edge or corner point, (*x, y, z*), due to the noise.

(b) The noise spatial distribution over an edge line is considered as one sample of a pseudo random variable. Each time this pseudo random variable takes a vector of values, including the mean and variance for the noise spatial distribution. The statistical measures of this pseudo random variable include its mean, which is actually the mean of a set of spatially-distributed noise values, and its variance, which is the variance of the same noise set.

Assume that *n* rounds of measurement are conducted. An average spatial distribution of measurement noise can be obtained by using the following formula:

$$(\bar{x}, \bar{y}, \bar{z}) = \sum_{i=1}^{n} \left((x_i, y_i, z_i) + (e_{x_i}, e_{y_i}, e_{z_i}) \right) / n\,, \tag{2}$$

where $(\bar{x}, \bar{y}, \bar{z})$ refers to the average perturbed position vector at the edge point, (*x, y, z*), over all the measurement (*n* times). (x_i, y_i, z_i) and $(e_{x_i}, e_{y_i}, e_{z_i})$ represent the values at the *i*-th measurement. Figure 4 shows the result of a typical measurement sample. The spatial distribution of measurement noises at sharp edges is illustrated in Figure 5. The measurement noise at a sharp edge is quantified by two components: $|\mathbf{e}|$ and ϕ, where $|\mathbf{e}|$ is the magnitude of noise and ϕ refers to the orientation angle of the edge noise vector with respect to the local cylindrical coordinate (x_L, y_L), as shown in Figure 4(b). Note the axis of this cylindrical coordinate system is in the same direction as the edge line. As

you can see in Figures 5 and 6, the noise magnitude distribution is close to an exponential distribution with waviness in the range of edge line, and is of the similar pattern with each measurement round. An approximate uniform distribution with waviness is observed for the orientation angle ϕ of measurement noises. Note that the spatial distribution here is simplified to the probability density distribution of a one-dimensional series of noise values.

The computation of the mean and variance of the pseudo random variable provides the statistical information about a typical spatial distribution of measurement noises. Note that the mean and variance here refer to the statistical nature of the overall measurement on the edge line. The consideration at a finer spatial scale will be given in Table 1 in the next section.

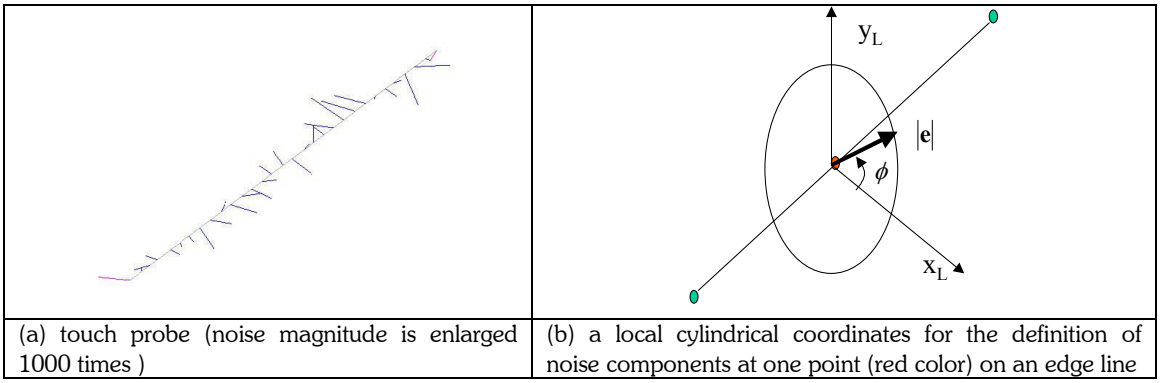

(a) touch probe (noise magnitude is enlarged 1000 times)

(b) a local cylindrical coordinates for the definition of noise components at one point (red color) on an edge line

Fig. 4: Typical spatial distribution of measurement noise at a sharp edge.

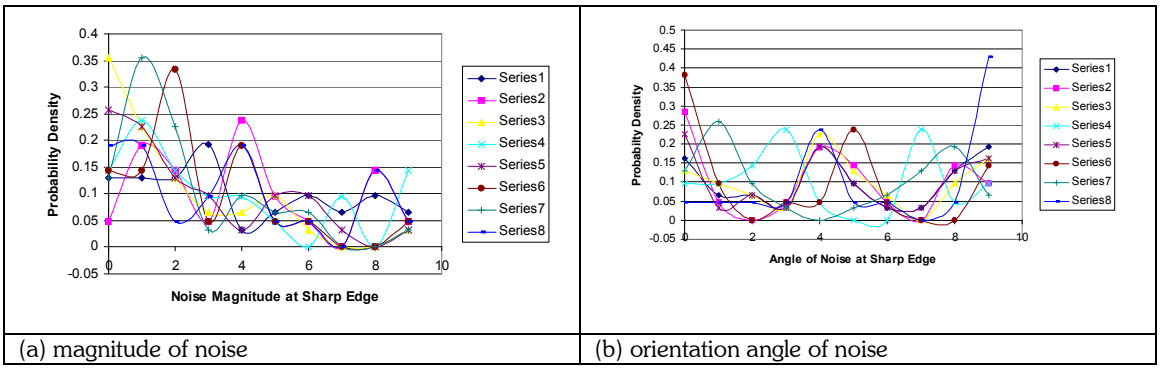

(a) magnitude of noise

(b) orientation angle of noise

Fig. 5: Probability density distribution of measurement noises at sharp edges with the touch probe.

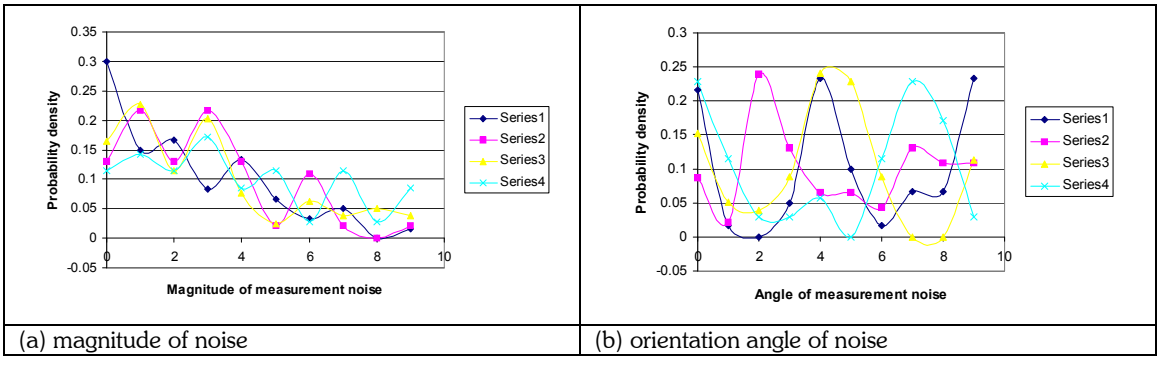

(a) magnitude of noise

(b) orientation angle of noise

Fig. 6: Probability density distribution of measurement noises at sharp edges with the laser sensor.

4. MEASUREMENT NOISE TEMPLATE AT SHARP EDGES

We propose a Statistical Binary Tree (SBT) as a measure to quantify the spatial distribution of measurement noise over the edge line to a reasonable degree. The basic idea of SBT is to subdivide the edge line by a binary tree that has a limited depth bound. In this way, the subdivision process does not proceed in an unlimited way down to the level of edge vertex. As a matter of fact, it will terminate at certain level at which the statistical properties (mean and variance) of the spatial distribution over each subdivided line segment are computed and used to represent the spatial distribution over the subdivided segments in a statistical sense. Figure 7 illustrates the subdivision process in creating such a SBT, and the detailed procedures for doing so are listed in Table 1.

The subdivision process is controlled by the following two termination criteria:

$$N_{sub} > N_t \qquad \sigma < \sigma_t \,, \tag{3}$$

where N_t and σ_t are the limit for maximum subdivision steps and a threshold for variance of measurement noise over a subdivided segment, respectively. N_{sub} and σ are subdivision steps and variance of measurement noise for each subdivided line segment, respectively. If there is no measurement noise in a certain segment, then this is a special case with zero variance and there is no need for any further subdivision in it. The choice of σ_t has a direct influence on the topology of SBT. If σ_t is set to be higher than the variance, σ_0, of measurement noise in the initial edge line, then the SBT contains only a root node, indicating a uniform distribution over the line region. In this study, we set $\sigma_t = ts \times \sigma_0$, where ts is a threshold scale that is less than unity.

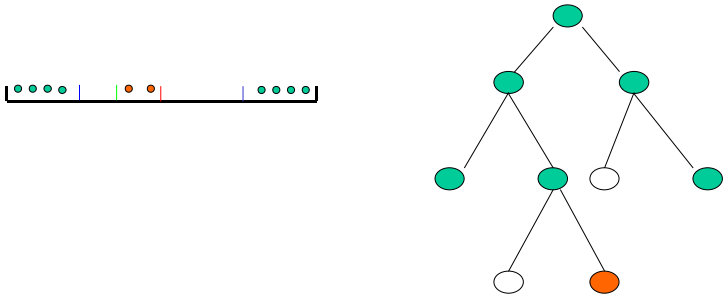

(a) an edge line on which some noises (green or red dots) exist

(b) statistical binary tree

Fig. 7: Creation of a SBT. (Empty node represents an empty segment; The sequence of two binary segments in a subdivision is 1) left, and 2) right.)

(1)	start from an edge line region as the current line segment in the parametric domain and set $N_{sub} = 1$
(2)	compute the mean and variance of measurement noise in the current segment
(3)	create a SBT node in the statistical binary tree
(4)	if the variance is less than σ_t, stop the current branch of subdivision process. Otherwise, subdivide the current segment into two smaller ones
(5)	if $N_{sub} = N_t$, stop the subdivision process. Otherwise, $N_{sub} = N_{sub} + 1$ and repeat steps (2) through (5)

Tab. 1: Procedures for creating a SBT by a subdivision process.

The structure of each SBT represents the spatial distribution of different segments over the edge line region, and the variance of measurement noise over each segment is less than a predetermined threshold or the size of the segment already reaches the subdivision limit. The statistical values at each node of the SBT refer to the statistical properties (mean and variance) of each segment. Thus, the tree structure and nodal values in our SBT are two basic components to describe the spatial distribution in a hybrid deterministic and statistical way, which reflects a tradeoff between the accuracy and computational efficiency. In summary, SBT is a special binary tree in which each node has the values of mean and variance.

The SBT represents a measurement noise template at sharp edges. However, the mean and variance at each leave are meaningful only in the sense of statistics. It is impossible to find an accurate noise perturbation in a deterministic way at each edge point in the parametric space on the basis of the resulting measurement noise template. On the other hand, it still effectively provides some sort of spatial distribution information, which is sufficient for the measurement noise synthesizer in the next section.

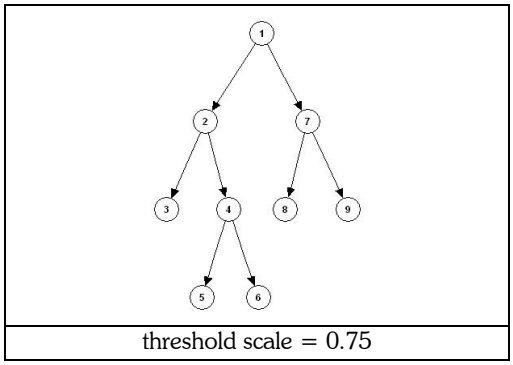

Fig. 8: Spatial distribution noise template for a touch-probe.

5. SYNTHESIZER FOR MEASUREMENT NOISE AT SHARP EDGES

A synthesizer for measurement noises is defined as a simulator that produces a measurement noise distribution synthetically. In the cases of sharp edges, its key component is the synthetic reconstruction of measurement noise pattern over an edge line region with a measurement noise template (SBT) available, as described in Table 2.

Since the angle and magnitude are two components for the measurement noise distribution along a line segment, they need to be handled separately. On the basis of Figures 5(b) and 6(b), a uniform distribution can be used to approximate the probability distribution of angles along the edge. Therefore, there is no need for SBT to represent the distribution of angles. A random number generator can be directly used to cover a uniform distribution of angles from 0 to 360 degrees. On the other hand, the magnitude does not follow a uniform distribution, as illustrated in Figures 5(a) and 6(a). Thus, the magnitude distribution along the edge is described by a SBT tree in which each node has its nodal values (mean and variance). A random number generator can be used with a suitable scaling to generate the desired mean and variance over each segment of SBT. The random number generator is initiated with a different seed number for different segments of SBT. The scaling of a series of random numbers includes two steps:

1) scale the variance of the numbers to the variance of the SBT segment

$$x_i = \bar{x} + (x_i - \bar{x}) \times s_\sigma \ (i = 0, \ldots, n) , \tag{4}$$

where $s_\sigma = \sqrt{\frac{\sigma_q}{\sigma_r}}$, in which σ_r and σ_q are the variances of the random numbers and the SBT segment, respectively. $\bar{x}$ is the mean of the random number set.

2) translate the mean of the numbers to the mean of the SBT segment.

$$x_i = x_i - \bar{x} + \bar{y} \ (i = 0, \ldots, n) , \tag{5}$$

where $\bar{y}$ refers to the mean of SBT segment.

The procedures presented above work only partially well, because x_i in Equation (5) may turn to be negative, which is not allowed for the magnitude. Therefore, a procedure is designed in Table 3 to make all x_i positive and in the meantime to maintain the original mean and variance of the series $\{x_i\}$. The precondition for the procedure in Table 3 to be correct is that there should be only very few negative numbers in $\{x_i\}$. This is true for the case of edge noise magnitude. One negative number out of thirty positive numbers was observed with $\bar{y}$ and σ_q specified in the SBT. The basic idea of steps (5) and (6) in Table 3 is that each y_j is brought back to zero, and in the meantime z_j is changed to $z_j - \Delta$ in order to maintain the mean of $\{x_i\}$. However, the movement of this pair $\{y_j \quad z_j\}$ causes a change, δ_σ, in the variance of $\{x_i\}$:

$$\delta_\sigma = (y_j - \bar{x})^2 - (0.0 - \bar{x})^2 + (z_j - \bar{x})^2 - (z_j - \Delta - \bar{x})^2 , \quad (6)$$

where $\bar{x}$ is the mean of $\{x_i\}$, and $\Delta = -y_j$ represents the movement amount of the pair $\{y_j \quad z_j\}$. $\{y_j\}$ is a list that contains n_neg elements which are all the negative numbers in $\{x_i\}$, while $\{z_j\}$ is a list that contains n_neg elements whose values are the greatest in $\{x_i\}$ and greater than $\bar{x}$, the mean of $\{x_i\}$. In order to cancel the variance change, δ_σ, the movement of another pair, $\{up_j \quad down_j\}$ is needed. Here, $\{up_j\}$ is a list that contains n_neg elements whose values are around $\bar{x}$, and greater than $\bar{x}$; $\{down_j\}$ is a list that contains n_neg elements whose values are also around $\bar{x}$, but smaller than $\bar{x}$. The movement amount, t, of the second pair is determined by the following equation

$$(up_j - t - \bar{x})^2 - (up_j - x)^2 + (down_j - t - \bar{x})^2 - (down_j - \bar{x})^2 = \delta_\sigma , \quad (7)$$

which can be converted to a quadratic equation of t

$$t^2 + (up_j - down_j)t - 0.5\delta_\sigma = 0 . \quad (8)$$

One smaller positive root of this equation is used to compute the movement amount for the pair $\{up_j \quad down_j\}$.

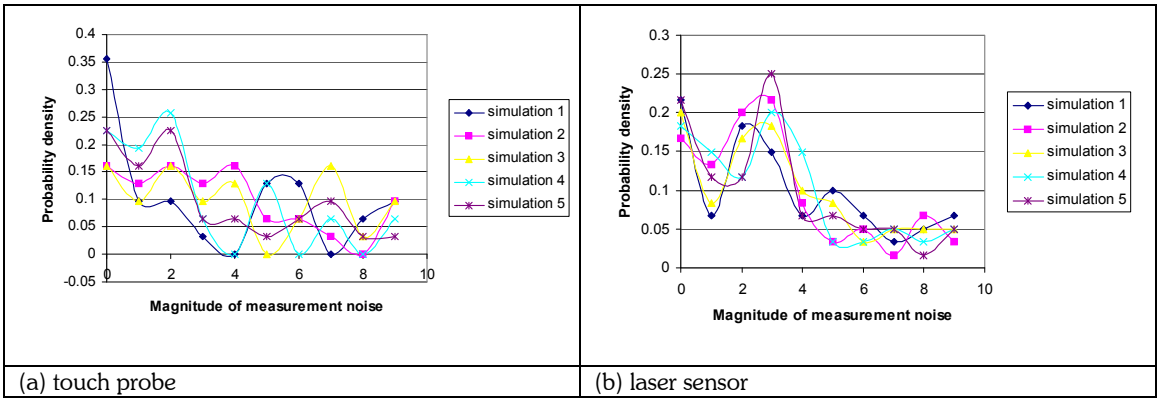

(a) touch probe (b) laser sensor

Fig. 9: The probability density curves of synthesized edge noises.

In order to compare how close the measurement noise generated by the synthesizer described in Table 2 is to the real measurement noise, the probability density curves of synthesized edge noises are given in Figure 9. These curves are quite similar to those of real measurement noises in Figures 5(a) and 6(a), indicating the effectiveness of our approach. In addition, first four central moments of overall noise distribution on the edge line region are computed, and listed in Tables 4 and 5. It can be seen from these two tables that the difference between the synthesized and real noise distributions is not significant if SBT structure is used (cases 2 and 3). On the other hand, the third and fourth moments in cases 4 and 5 (without an effective use of SBT structure) are noticeably different from those in case 1 in these two tables. Therefore, the synthesizer proposed in this paper can be used to substitute a real measurement noise distribution at sharp edges for comparing different denoising algorithms. Note that the results in Tables 4 and 5 are with respect to the noise magnitude at sharp edges. Since the magnitude approximately follows an exponential distribution, we might use this reason to infer why case 3 provides a slightly better result than case 2 in these two tables.

The reconstructed noise distribution over a line region can be mapped onto an arbitrary sharp edge by linear interpolation. Since the spatial distribution along sharp edges and corners is different from that in a surface domain. The detailed procedure for the noise template mapping is as follows:

(1) noise template mapping within smooth surface regions
(2) noise template mapping along sharp edges
(3) noise template mapping at sharp corners

Each of the above steps may override the content produced at a previous step.

1. Construct noise angle distribution, $\{\phi_i\}$, by a random number generator, which ranges from 0 to 2π
2. Generate noise magnitude distribution, $\{|\mathbf{e}_i|\}$, with a given SBT
   - 2.1 Partition a line region by all the leaves in a given SBT
   - 2.2 Loop over each partition
   - 2.3 Generate a different seed number for each partition
   - 2.4 Construct noise perturbation by a random number generator controlled by the mean and variance of the corresponding tree node
   - 2.5 Repeat steps 2.2 through 2.4
3. Calculate the overall synthetic edge noise by

   $x_i = |\mathbf{e}_i| \sin\phi_i$, $y_i = |\mathbf{e}_i| \cos\phi_i$,

   where x_i and y_i refer to the local coordinates that are perpendicular to the edge line. z_i is the local coordinate along the edge line.

Tab. 2: Synthesizing Measurement Noise Distribution at a Sharp Edge.

(1) Loop over an input series $\{x_i\}$ to determine a list $\{y_j\}$ that contains n_neg elements which are all the negative numbers in $\{x_i\}$

(2) Create a list $\{z_j\}$ that contains n_neg elements whose values are the greatest in $\{x_i\}$ and greater than $\bar{x}$, the mean of $\{x_i\}$

(3) Create a list $\{up_j\}$ that contains n_neg elements whose values are around $\bar{x}$, but greater than $\bar{x}$

(4) Create a list $\{down_j\}$ that contains n_neg elements whose values are around $\bar{x}$, but smaller than $\bar{x}$

(5) For each j,

$\Delta = -y_j$

$\delta_\sigma = (y_j - \bar{x})^2 - (0.0 - \bar{x})^2 + (z_j - \bar{x})^2 - (z_j - \Delta - \bar{x})^2$

solve a quadratic equation, $at^2 + bt + c = 0$, where $a = 1.0$, $b = up_j - down_j$, and $c = -\delta_\sigma / 2.0$

(6) Update the number in $\{x_i\}$, which corresponds to up_j, by $up_j + t$

Update the number in $\{x_i\}$, which corresponds to $down_j$, by $down_j - t$

Update the number in $\{x_i\}$, which corresponds to y_j, by 0.0

Update the number in $\{x_i\}$, which corresponds to z_j, by $z_j - \Delta$

(7) Repeat steps (5) and (6) for each j

Tab. 3: Correction of a Random Number Series for Magnitude of Edge Noise.

6. CONCLUDING REMARKS

In this paper, we explored the spatial distribution problem of measurement noise at sharp edges. Two components, magnitude and angle, are used in the representation of noise distribution. It was observed that the distribution of noise magnitude at sharp edges follows some kind of exponential distribution with waviness, while the angle distribution can be approximated by a uniform distribution with waviness. The concept of statistical binary tree (SBT) is used to represent the spatial distribution of measurement noise magnitude at sharp edges, while a random number generator is directly used for the angle distribution. A procedure has been proposed to synthesize the measurement noises at sharp edges on the basis of SBT. The probability density distribution of the synthesized noises is very close to that of measurement noises, indicating the effectiveness of our approach.

7. ACKNOWLEDGEMENT

This paper was supported by USA NSF DMI 0514900

cases	mean	standard deviation	skewness	kurtosis
1. Real measurement noise	69.9	40	0.3003	-1.1286
2. Synthetic noise reconstructed from SBTnode through system-supplied random number generator in ANSI C	69.9	40	0.0535	-1.2424
3. Synthetic noise reconstructed from SBTnode through exponential deviates	69.9	40	0.1288	-1.3806
4. Synthetic noise reconstructed from the root node of SBT tree through system-supplied random number generator in ANSI C	69.9	40	-0.2084	-1.5771
5. Synthetic noise reconstructed from the root node of SBT tree through exponential deviates	69.9	40	1.3249	0.9279

Tab. 4: Reconstruction accuracy of noise template in global statistical property with the Renishaw touch probe (unit: micrometer).

cases	mean	standard deviation	skewness	kurtosis
1. Real measurement noise	120.8	98.9	0.8983	0.2962
2. Synthetic noise reconstructed from SBTnode through system-supplied random number generator in ANSI C	120.8	98.9	0.7503	-0.0797
3. Synthetic noise reconstructed from SBTnode through exponential deviates	120.8	98.9	0.9185	0.0281
4. Synthetic noise reconstructed from the root node of SBT tree through system-supplied random number generator in ANSI C	120.8	98.9	-0.0047	-1.5596
5. Synthetic noise reconstructed from the root node of SBT tree through exponential deviates	120.8	98.9	3.2485	11.61

Tab. 5: Reconstruction accuracy of noise template in global statistical property with the LDI laser probe (unit: micrometer).

8. REFERENCES

[1] Perona, P.; Malik, J.: Scale-space and edge detection using anisotropic diffusion, IEEE Transactions on Pattern Analysis and Machine Intelligence, 12(7), 1990, 629-639.

[2] Tomasi, C.; Manduchi, R.: Bilateral filtering for gray and color images, Proceedings of IEEE ICCV, 1998, 836-846.

[3] Fleishman, S.; Drori, I.; Cohen-Or, D.: Bilateral mesh denoising, Proceedings of the 30th Annual Conference on Computer Graphics and Interactive Techniques, 2003, 950-953.

[4] Choudhury, P.; Tumblin, J.: The trilateral filter for high contrast images and meshes, Christensen, Per. H. and Cohen, D. Proceedings of the Eurographics Symposium on Rendering, 2003, 186-196.

[5] Ohtake, Y.; Belyaev, A.; Seidel, H.: Mesh smoothing by adaptive and anisotropic Gaussian filter, Vision, Modeling, and Visualization 2002, 203-210.

[6] Clarenz, U.; Diewald, U.; Rumpf, M.: Anisotropic geometric diffusion in surface processing, Proceedings of IEEE Visualization, 2000, 397-405.

[7] Desbrun, M.; Meyer, M.; Schroder, P.; Barr, A. H.: Anisotropic feature-preserving denoising of height fields and bivariate data, Graphics Interface, 2000, 145-152.

[8] Bajaj, C.; Xu, G.: Anisotropic diffusion of subdivision surfaces and functions on surfaces, ACM Transactions on Graphics, 22(1), 2003, 4-32.

[9] Meyer, M.; Desbrun, M.; Schroder, P.; Barr, A. H.: Discrete differential-geometry operators for triangulated 2-manifolds, In Visualization and Mathematics III, 2003, 35-57.

[10] Tasdizen, T.; Whitaker, R. T.; Burchard, P.; Osher, S.: Anisotropic geometric diffusion in surface processing, IEEE Visualization 2002, 125-132.
[11] Zhang, H.; Fiume, E. L.: Mesh smoothing with shape or feature preservation, In. (Ed. J. Vince and R. Earnshaw), 2002, 167-182.
[12] Jones, T. R.; Durant, F.; Desbrun, M.: Non-iterative, feature-preserving mesh smoothing, Proceedings of the 30th Annual Conference on Computer Graphics and Interactive Techniques, 2003, 943-949.
[13] Hildebrandt, K.; Polthier, K.: Anisotropic filtering of non-linear surface features, Computer Graphics Forum, 23(3), 2004, 391-400.
[14] Shen, Y.; Barner, K. E.: Fuzzy vector median-based surface smoothing, IEEE Transactions on Visualization and Computer Graphics, 10(3), 2004, 266-277.
[15] Shen, J.; Maxim, B.; Akingbehin, K.: Accurate Correction of Surface Noises of Polygonal Meshes, International Journal for Numerical Methods in Engineering, 64(12), 2005, 1678-1698.
[16] Smith, K. B.; Zheng, Y. F.: Accuracy analysis of point laser triangulation probes using simulation, ASME Journal of Manufacturing Science and Engineering, 120(4), 1998, 736-745.
[17] Curless, B.; Levoy, M.: Better optical triangulation through spacetime analysis, Proceedings of IEEE International Conference on Computer Vision '95, 1995, 987-994.
[18] Cederberg, P.; Olsson, M.; Bolmsjo, G.: Virtual triangulation sensor development, behavior simulation and CAR integration applied to robotic arc-welding, Journal of Intelligent and Robotic Systems, 35(4), 2002, 365-379.